oceans

MDPI

Article

Hemispherical Distribution of Antarctic Krill Indicates High Abundance in Amundsen Sea

Molly Thornborrow [1], Andrew S. Brierley [2,†], Roland Proud [2], Inigo Everson [3], Joshua M. Lawrence [4], Matteo Bernasconi [2,5] and Paul G. Fernandes [4,*]

[1] School of Biological Sciences, University of Aberdeen, Aberdeen AB24 2TZ, UK; molly.thornborrow@sky.com
[2] Pelagic Ecology Research Group, Gatty Marine Laboratory, Scottish Oceans Institute, School of Biology, University of St Andrews, St Andrews KY16 8LB, UK; rp43@st-andrews.ac.uk (R.P.); matteo@whalesandco.com (M.B.)
[3] School of Environmental Sciences, University of East Anglia, Norwich Research Park, Norwich NR4 7TJ, UK; ideverson@gmail.com
[4] The Lyell Centre, Heriot-Watt University, Research Avenue South, Edinburgh EH14 4AP, UK; joshua.lawrence@hw.ac.uk
[5] Whales & Co. LLC, 3150 Harbor Blvd, Oxnard, CA 93035, USA
* Correspondence: p.fernandes@hw.ac.uk
† Deceased 19 February 2024.

Abstract

Antarctic krill (*Euphausia superba*) are an essential source of food for whale, seal, several fish, squid and seabird species in the Southern Ocean. Krill also play a major role in biogeochemical cycling and are the target of a growing commercial fishery. Krill can be detected and quantified with echosounders, particularly in swarms, and monitoring krill abundance and distribution is integral to assessing the status of regional populations and managing fisheries. We used echosounders to investigate the hemispherical distribution and behaviour of krill swarms during the Antarctic Circumnavigation Expedition (ACE), a multidisciplinary exercise that included measurements of atmospheric chemistry. Krill swarms were grouped using hierarchical clustering into four principal types: small swarms (on average 2 m high, 25 m long); large swarms (13 m high and 341 m long); deep swarms, which were also densely packed (average depth of 52 m); and shallower swarms, which had lower densities (average depth of 28 m). We found a weak negative relationship between the concentration of atmospheric methane close to the sea surface and the presence of krill. High densities of krill were found in the Amundsen Sea, an area purported to be of increasing importance for krill as the climate changes.

Keywords: krill; spatial distribution; acoustics; Southern Ocean; swarm structure; methane

check for updates

Academic Editor: Diego Macías

Received: 10 March 2025
Revised: 25 July 2025
Accepted: 12 September 2025
Published: 2 October 2025

Citation: Thornborrow, M.; Brierley, A.S.; Proud, R.; Everson, I.; Lawrence, J.M.; Bernasconi, M.; Fernandes, P.G. Hemispherical Distribution of Antarctic Krill Indicates High Abundance in Amundsen Sea. *Oceans* **2025**, *6*, 63. https://doi.org/10.3390/oceans6040063

Copyright: © 2025 by the authors. Licensee MDPI, Basel, Switzerland. This article is an open access article distributed under the terms and conditions of the Creative Commons Attribution (CC BY) license (https://creativecommons.org/licenses/by/4.0/).

1. Introduction

Antarctic krill (*Euphausia superba*) are pelagic crustaceans native to the Southern Ocean. Krill are at the hub of Southern Ocean food webs and act as a conduit for the transfer of energy from primary producers to higher trophic levels [1]. Antarctic krill are so abundant that they not only support some of the largest mammals on the planet, but they are also the subject of a substantial fishery, with 390,195 tonnes harvested in 2019 [2]. Krill are sought as a source of human food supplements and as meal for farmed fish [3]. In keeping with global trends for developing ecosystem-based fisheries management, the Commission for the Conservation of Antarctic Marine Living Resources (CCAMLR) has pioneered the development of an ecosystem approach to management, such that catch limits for krill

account for the needs of dependent predators [4]. CCAMLR's long-term strategy is to continually adjust management measures in response to estimates of the abundance of krill [2], which emphasises the positive impact that studying these animals has on their management and conservation. The use of acoustic surveys allows the abundance and distribution of this species to be determined in a practical and efficient manner, due largely to their habit of swarming.

Krill exhibit aggregative behaviour and congregate in daylight hours into swarms—this is the fundamental unit of krill biology [5]. Swarming behaviour has numerous potential benefits for the individual, including predator evasion [6] and food location [7]. Antarctic krill have both land-based and open-water predators. During colder months, krill depend greatly on the sea-ice microbial community to optimise their growth rates. Krill are, therefore, often distributed close to sea-ice and, in some locations, to land-based predators [8] that use sea-ice for breeding and resting. Krill also have many open-water predators, which include different species of whales, fish, and squid. Nowacek et al. (2011) found extremely high densities of humpback whales close to 'super-aggregations' of Antarctic krill [9]. They also found that tagged humpbacks rested during the day and fed at night when the krill were nearer to the surface, taking advantage of their prey's diurnal migratory behaviours.

Krill distribution has been shown to alter with season [10], with biomass on the shelf to the west of the Antarctic Peninsula being an order of magnitude higher in spring and summer than in autumn and winter. Given this seasonal variation, rising global temperatures are likely to affect the extent of their distributions, largely through changes in sea-ice cover, which would, in turn, affect sea-ice algae, one of krill's primary food sources. Piñones and Federov [11] made predictions of future changes in krill distribution due to climate change affecting sea-ice and chlorophyll *a*. Their predictions indicate that the western Weddel Sea, isolated areas of the Indian Ocean, and the Amundsen/Bellinghausen Sea will support successful spawning habitats for krill. This last region does not support successful krill spawning at present, and may, therefore, open up as a potential new habitat. There has been a small but statistically significant increase in Southern Ocean sea-ice over the last 37 years [12], so it is important to maintain large-scale measurements of krill distribution.

Advection, the bulk movement of water masses, along with the organisms present in these water masses, is another key driver of the large-scale distribution of Antarctic krill [13]. The Antarctic Circumpolar Current (ACC) is responsible for a lot of this bulk transport. The southernmost boundary of the ACC provides a productive foraging ground for krill due to the high phytoplankton biomass there, which further influences krill distribution [7]. Alongside this large-scale movement, studies have shown that individual locomotion of Antarctic krill is also vital in the maintenance of large swarms [14].

The categorisation of krill swarms can determine if there are broad characteristics that swarms possess. Linking the categories to different variables may help us to understand krill ecology and distribution. A number of different approaches for categorising krill swarms have been taken. For example, Krafft et al. [15] categorised the swarms into four key groups with varying size and depth distribution, whereas Tarling et al. [16] primarily used packing concentration and morphological dimensions to group swarms. Tarling et al. [16] categorised the swarms that they observed into two main groups: Type 1 swarms were small and not very densely packed, whereas Type 2 swarms were a lot larger and much more densely packed [16]. Each of these groups were then further divided into two subtypes based on size. Another group (Type 3) was identified but was much less frequently observed; these swarms were located more than 100 km away from other swarms and were, therefore, labelled as "isolated". There are many factors, both internal and external, that can affect the characteristics of Antarctic krill swarms. Tarling et al. [16] found a

relationship between the type of swarm and surface fluorescence, photosynthetically active radiation (PAR), krill maturity, and krill body length [16]. They concluded that the structure of swarms alters from being mainly large and tightly packed to smaller and less tightly packed as the krill mature. However, Tarling et al. [16] stated that there are further variables that alter this trend, including food availability and light level.

Traditionally, krill populations would have been monitored with net-based sampling systems [17–20]. However, the use of echosounders to provide estimates of abundance and distribution at a high spatial resolution has increased over the past few decades [6,21]. Scientific echosounders (hereafter referred to only as "echosounder/s" for brevity) have electronics built in to deliver signals with high precision and come with facilities to calibrate and adapt the devices for accurate scientific output [22]. Alongside these systems, nets can be used to provide alternative evidence to confirm the species, as well as additional information such as the size and maturity of the individual targets.

In 2016–2017, the Antarctic Circumnavigation Expedition (ACE) took place to study the Southern Ocean ecosystem. This was a multidisciplinary cruise, which included over 20 studies of atmospheric, marine and terrestrial physics, chemistry, and biology. One of these studies comprised an acoustic survey, intended to study mesopelagic fish, but in so doing, also collected data on Antarctic krill swarms. Another of the studies provided a survey of atmospheric methane close to the sea surface. We aimed to use the extensive geographic coverage of both of these surveys to provide a hemispherical distribution of krill in the Southern Ocean between longitudes 178 W and 1 E (Figure 1) and determine if krill swarms contributed to atmospheric methane concentrations. Methane is a significant greenhouse gas that is usually produced in anoxic conditions. However, substantial amounts of methane are produced from oxygenated shallow marine systems, without adequate explanation, giving rise to the methane paradox [3]. Previous experiments in the laboratory [4] and field [5] have associated zooplankton with methane production. Making use of the interdisciplinary teams on ACE, we aimed to compare our highly spatially resolved continuous detections of krill swarms to the synchronous atmospheric methane measurements, which may help to explain part of the methane paradox in the Southern Ocean.

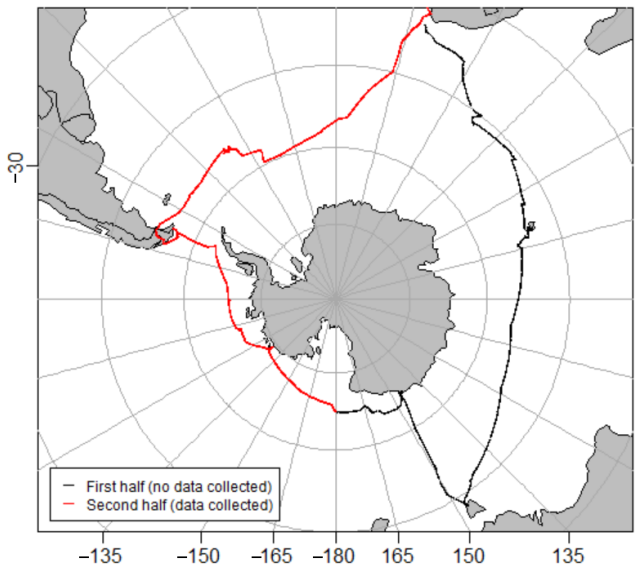


Figure 1. The route (black and red lines) of the R.V. Akademik Tryoshnikov during the ACE. Data allowing for the detection of krill (red line) were collected in an area from Scott Island (located at 180° W) on 7 February 2017 to Cape Town, South Africa, on 18 March 2017. Latitudes and longitudes expressed as negative degrees for west and south.

Having not had access to net-based systems to provide alternative evidence for the acoustically detected krill swarms, one of the objectives of the analysis conducted here was to compare the statistics derived from the swarms in this study with the published values to provide further evidence that the swarms that we detected were Antarctic krill. The properties of the swarms detected were grouped into different swarm types based on a variety of different swarm parameters and analysed in terms of their characteristics and spatial distribution. The methane concentration was then analysed in relation to the density of krill to determine whether there was a statistically significant relationship present.

2. Materials and Methods

Data were taken from the survey carried out by the Russian Research Vessel (RV) Akademik Tryoshnikov from 20 December 2016 to 18 March 2017. The survey was circumpolar, completing a total of 3 legs consisting of 16 island hops around the entire Southern Ocean (Figure 1). The vessel travelled at an average speed of 12 knots (6.17 $m \cdot s^{-1}$). The 200 kHz echosounder, required to detect krill, was operational from 7 February 2017 to 18 March 2017 beginning at Scott Island (67°23′ S, 179°55′ W) during the second leg of the trip (Figure 1). Leg 3 began at Punta Arenas, Chile, and ended at Cape Town, South Africa (33°55′ S, 18°25′ E).

2.1. Acoustic Data Collection and Processing

Acoustic data were collected using a Simrad EK80 echosounder (Kongsberg Discovery, Horten, Norway) connected to a hull-mounted 12.5 kHz transducer and a Simrad EK60 echosounder connected to a 200 kHz transducer. The calibration of both systems took place in Cumberland East Bay, King Edward Point, South Georgia, on 2 March 2017. Calibration followed the standard methods [23,24] using a tungsten carbide sphere with a 38.1 mm diameter.

No 'ground-truthing' of the acoustic data with net sampling was possible, and the method of dB-difference, which is normally used in surveys to identify krill echotraces [22], also could not be carried out. The lower-frequency transducer (12.5 kHz) was used with a long pulse length alongside the higher-frequency transducer (200 kHz) to enable sampling in deeper water and, as such, did not give the appropriate sample resolution; the 12.5 kHz frequency also had a very long transmit pulse, causing interference at the surface. Visual inspection of the data from the two frequencies did, however, allow for the different types of turbulence to be distinguished, such as that generated by wave action or the ship's thrusters, with these types having a stronger echo at lower frequencies (due to resonance created by air bubbles). After the turbulence was removed, inspection also allowed for large targets (echotraces) to be distinguished as putative krill swarms by the comparison of swarm echotraces between the two frequencies. The statistics of the putative swarms were then compared with the published values from krill swarms [16].

Raw acoustic data collected using the 12.5 kHz and the 200 kHz transducers (Figure 2a,b) were processed using Sonardata Echoview version 11.0.255 (Echoview Software Pty Ltd., Hobart, Australia). Background noise was excluded from both the 12.5 kHz and 200 kHz echograms using a filter (Figure 2c). A combination of masks and filters (including a median 3 × 3 filter; Figure 2d) were used to remove isolated scatterers and interference, which was primarily from other acoustic devices on the ship. The swarms were then detected and labelled using image analysis algorithms [25], producing the final post-processed output (Figure 2e). The visual difference between the high-frequency and low-frequency echograms was inspected to aid in distinguishing krill swarms from turbulence (Figure 3).

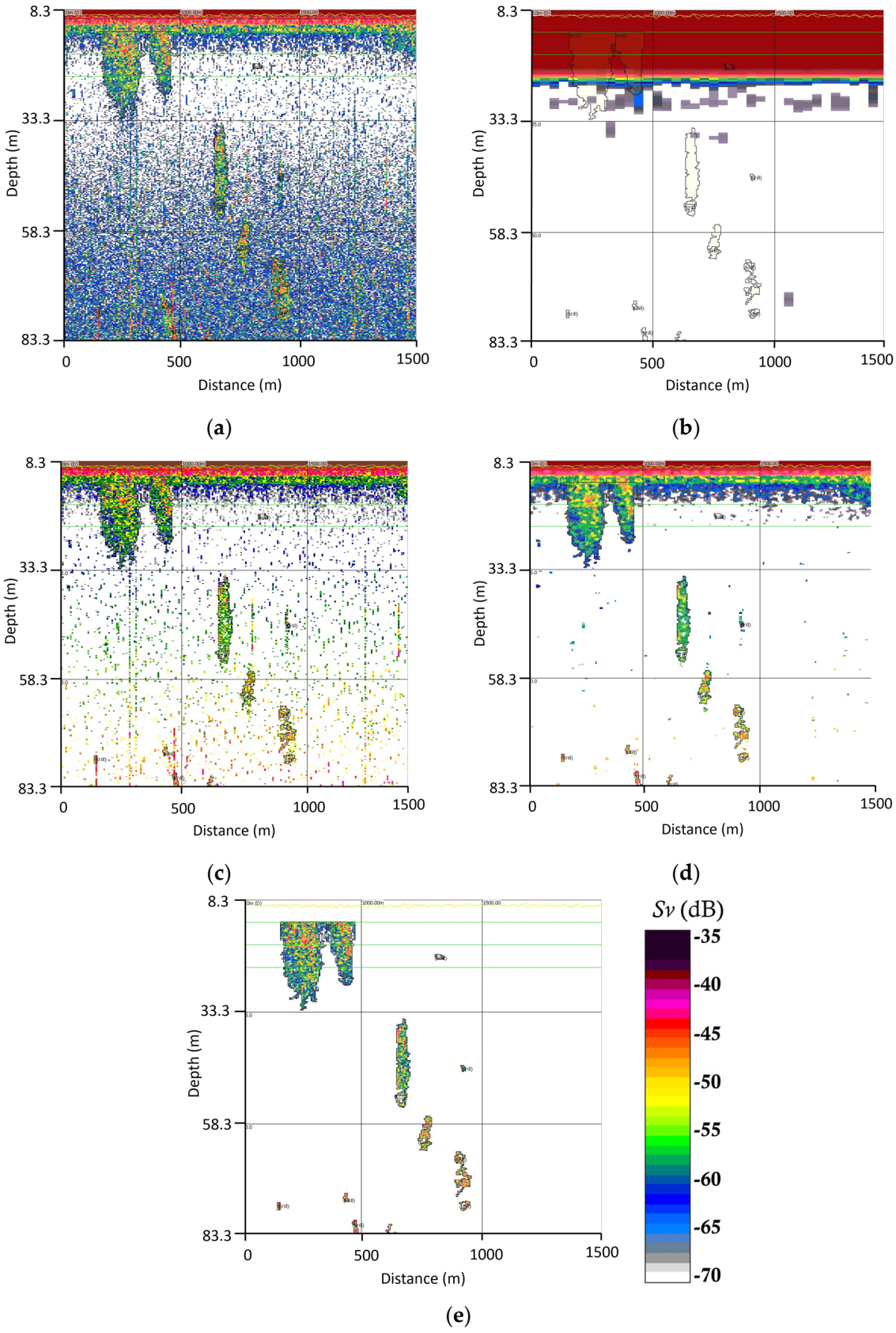


Figure 2. Echograms showing (**a**) 200 kHz raw *Sv* data, (**b**) 12.5 kHz raw *Sv* data, (**c**) background noise removal at 200 kHz, (**d**) median filter application at 200 kHz after which image analysis techniques were used to detect and label the krill swarms [25], and (**e**) final post-processed echotraces of krill swarms only. This data was collected on 7 February 2017, beginning at 10:42:20 and ending at 10:47:41. Note the depth on the Y axis, which begins at 8.3 m, the depth of the transducer below the sea surface.

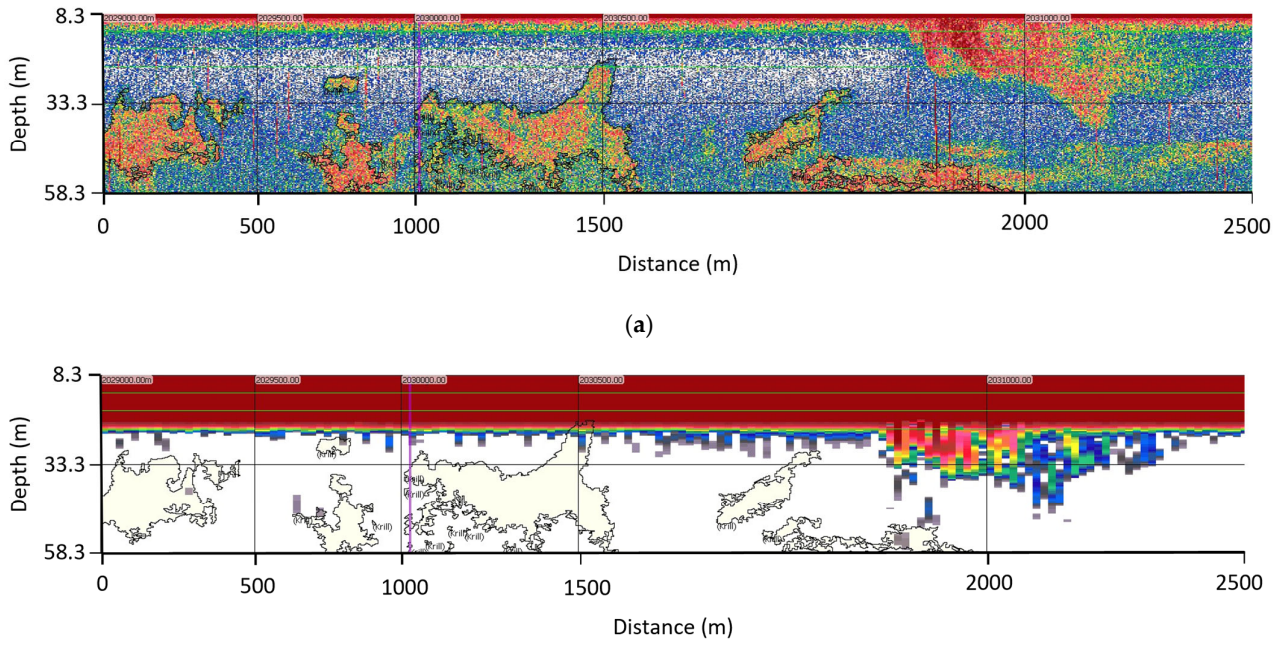


Figure 3. Echograms showing (**a**) 200 kHz raw *Sv* data and (**b**) 12.5 kHz raw *Sv* data on 12 February 2017 beginning at 05:51:46 and ending at 05:57:44. Krill swarms only appear on high-frequency echograms (**a**), shown by the black polygons on the lower-frequency echogram (**b**). At a depth of around 13–38 m and a distance along the transect of around 1900–2200 m, there is something that appears to be a krill swarm in the 200 kHz echogram (**a**); however, it is still present on the 12.5 kHz echogram (**b**), suggesting that it cannot be krill. The large gap between 1500 and 2000 m on the x axes of both echograms indicates that the boat had slowed down, and then, at around 1900 m, it accelerated again. This will have generated surface turbulence from the ships' thrusters, which was then picked up by both echosounders (at 1900–2300 m on both (**a**,**b**)), whereas the krill swarms were only detected at 200 kHz (**a**). Note that the depth on the Y axis begins at 8.3 m, as this is the depth of the transducer below the sea surface. Colour scale follows that of Figure 2.

2.2. Swarm Characteristics

The data were integrated [21] over the full depth surveyed (100 m) and exported from Echoview in two different forms: by swarm and by an Equivalent Distance Sampling Unit (EDSU) of 500 m. Each individual swarm was associated with several statistical characteristics, including mean swarm depth (m), thickness (vertical extent, m), length (horizontal extent, m), area (m^2), and perimeter (m), along with mean volume backscattering strength (S_v, dB). These data were then imported into the statistical programming language R (version 4.1.1), where, in addition to other analyses, the distance to the next swarm (km) was calculated using the distance along the transect for each swarm. Finally, two further swarm characteristics were calculated: packing concentration (N_v, ind·m^{-3}) and sum abundance (N_t, ind·m^{-1}). These calculations relied upon an estimation of the target strength (*TS*) of an individual krill, taken from the work of Tarling et al. [16] as −74.54 dB. The average body length of krill with a *TS* of −74.54 dB, using data provided in Tarling et al. [16], was 55 mm, whereas the body length of krill regurgitated by seabirds on the ACE (Figure S1) was 53 mm. N_v was estimated as

$$N_v = 10^{(Sv-TS)/10} \quad (1)$$

N_t was then calculated according to

$$N_t = N_v A \quad (2)$$

where A is the swarm mean area (m^2). This measure of abundance estimates the number of krill in a metre-thick slice of the swarm, hence the units (m^{-1}). This was favoured over estimating the total abundance of krill in the swarm due to the lack of information on the complex three-dimensional swarm features. The data was then examined to remove swarms that had extreme or impossible values based on graphical analysis. A total of 50 swarms were removed as they had values that were highly deviant from the rest of the data in one or more of the parameters assessed.

2.3. Statistical Comparison of Krill Swarm Characteristics

Statistics from previously identified krill swarms [16] were used in a comparison analysis with the data collected on the ACE to confirm that the latter were indeed krill swarms. An unpaired two-sample *t*-test was carried out to compare each of the swarm parameters (depth, thickness, length, area, distance to next swarm, packing concentration and sum abundance), along with Kolmogorov–Smirnov (KS) tests to determine whether the distributions were different. However, given the large sample size, *t*-tests could have detected differences in the means that were statistically, but not biologically, significant. To address this issue, a Cohen D test was used as an effect size statistic for a two-sample *t*-test to determine the extent of the differences between the means of each sample [26]. The relationship between swarm depth and packing concentration was investigated using linear regression.

2.4. Cluster Analysis

A hierarchical cluster analysis was performed using the Euclidean distance method [27] to confirm visual indications of the different types of krill swarms that were detected. The swarm characteristics previously mentioned were all used in the determination of the clusters. A $\log(x + 1)$ transformation was used on all variables to minimise the impact of extreme values.

2.5. Methane Data Collection and Analysis

Methane concentrations (ppm) were collected using an aerosol inlet from 15 m above the sea surface and a Picarro G2401 (Pincarro Inc., Santa Clara, CA, USA) gas analyser every minute from 17 December 2016 to 10 April 2017. Methane concentration data had to be matched with the krill data to determine the methane concentration per EDSU. Since the methane data were collected every minute consecutively throughout the course of the survey, an average methane concentration was generated for every kilometre across the transect. The methane concentration was then compared to krill density ($ind \cdot m^{-2}$) using a non-parametric Spearman rank correlation test.

2.6. Day/Night Analysis

The day/night effect was investigated by reference to the sun angle due to the nature of the cruise, which went through continually changing longitudes. The sun angle was calculated as a function of latitude and longitude using the 'suncalc' package in R. The sun angle was then examined in relation to the swarm characteristics.

3. Results

3.1. Swarm Characteristics

A total of 1741 krill swarms were detected. The mean swarm depth (i.e., the depth at which the swarm was detected) was 38.49 m (range 15.46–105.85 m). Swarm depths

showed a log-normal statistical distribution (Figure 4a). The thickness of all the swarms averaged 5.90 m (range 0.35–46.55 m). The $\log_{10}$ thickness shows a combination of two distributions: a normal and a right skew (Figure 4b). Tarling et al. [16] removed the thinner swarms; however, in this study, it was decided that they should not be removed due to the high frequency of small and thin swarms present. The mean swarm length was 115.96 m (range 0.12–6742.38 m) (Figure 4c). The mean swarm area was 875.54 m^2 (range 0.05–104,776.45 m^2). Most of these statistics displayed a relatively log-normal distribution; however, there is some evidence of bimodality, possibly due to the presence of different swarm types (Figure 4d). The mean distance to the next swarm was 5.79 km (range 0.003–661.07 km). The distribution of $\log_{10}$ distance to the next swarm was right-skewed, indicating that it was more common to find swarms closer to one another than further away (Figure 4e). Both swarm packing concentration and swarm sum abundance were log-normally distributed (Figure 4f,g). The mean packing concentration for all the swarms was 591.82 ind·m^{-3} (range 3.74–16,016.51 ind·m^{-3}) (Figure 4f). The sum abundance was, on average, 288,015.10 ind·m^{-1} (range 7.84–1.28 × 10^7 ind·m^{-1}) (Figure 4g).

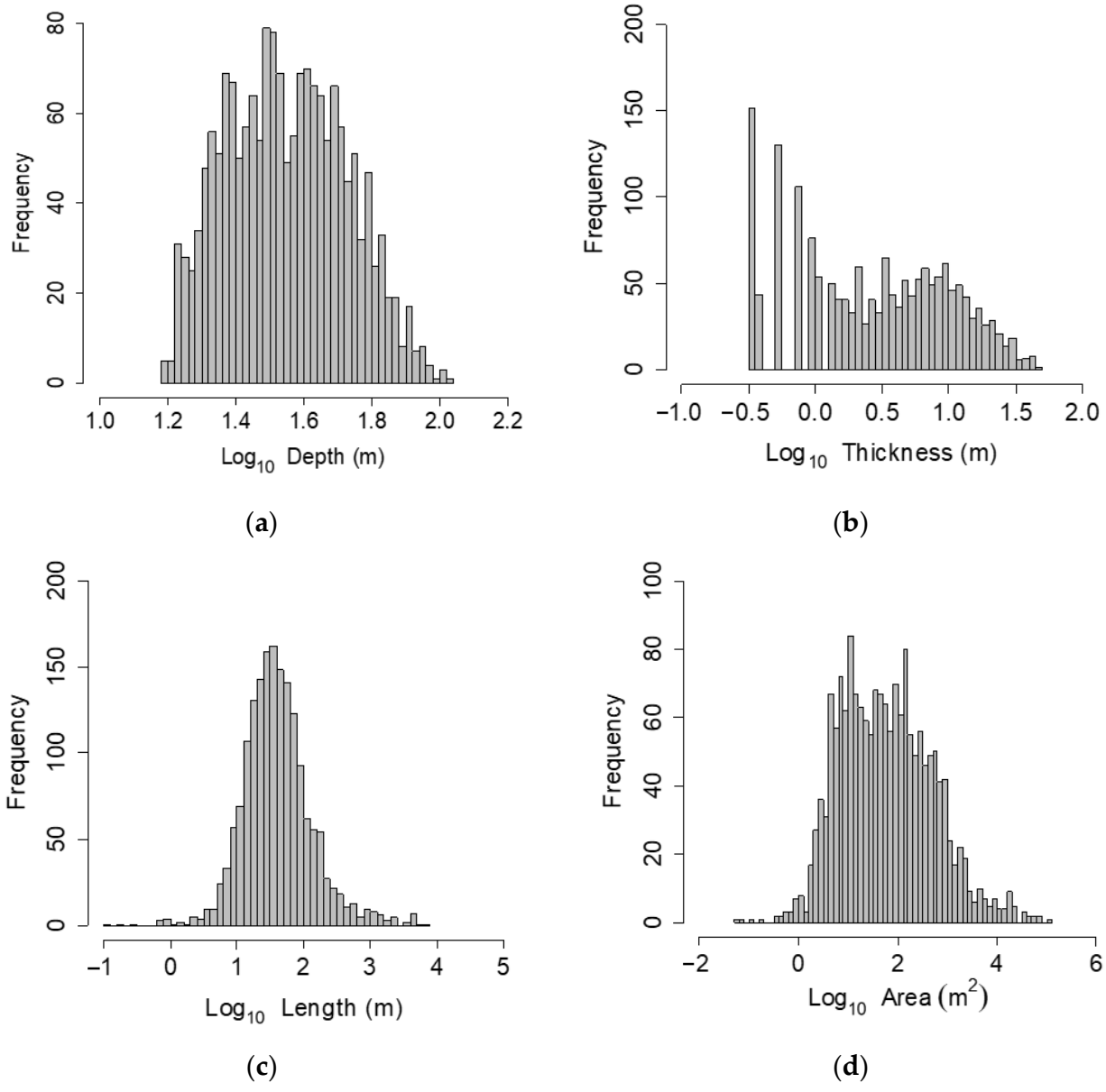


Figure 4. *Cont.*

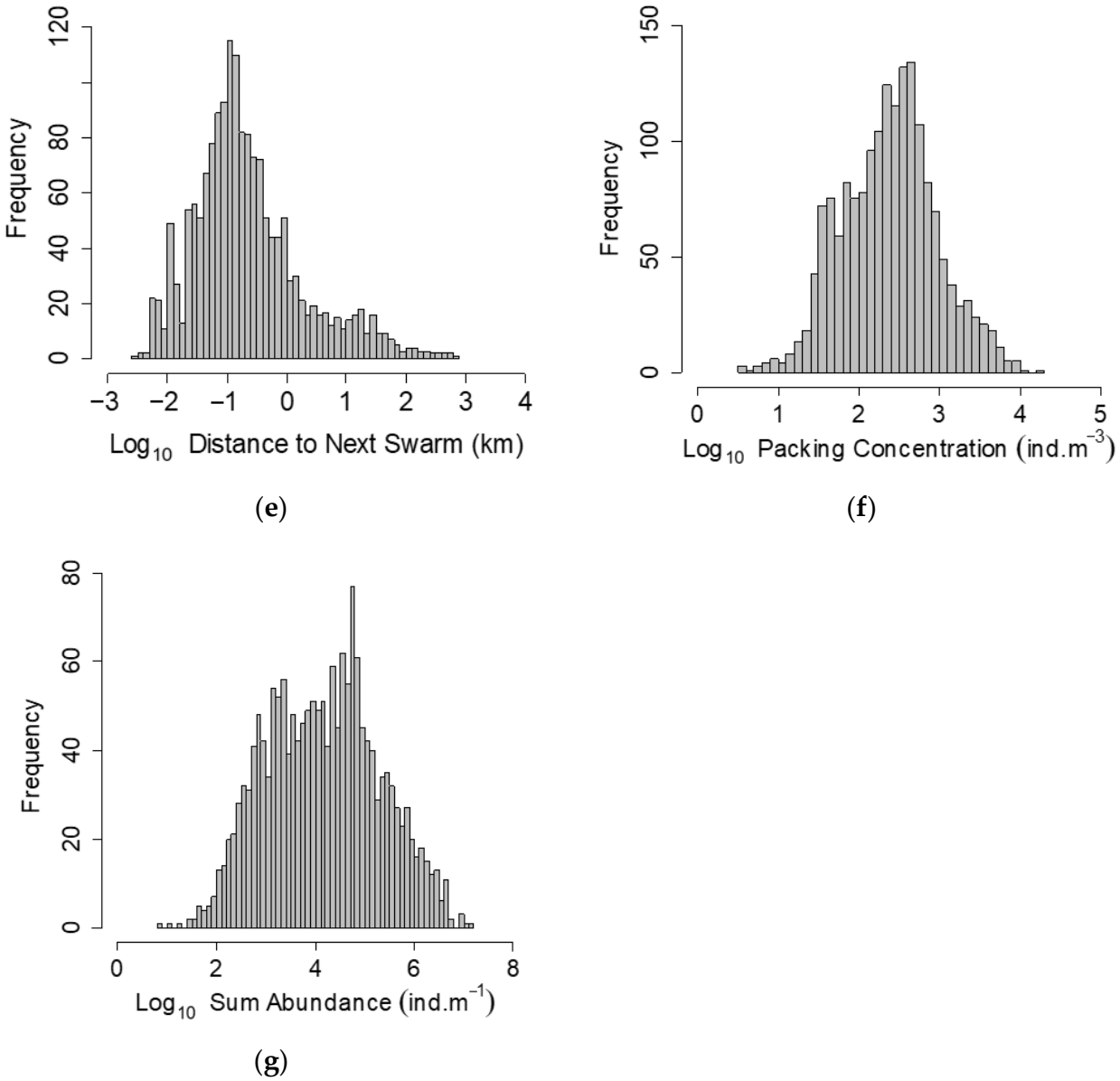


Figure 4. The frequency distribution of krill swarm parameters. Graphs show the frequency distribution of (**a**) swarm depth, (**b**) swarm thickness, (**c**) swarm length, (**d**) swarm area, (**e**) distance to next swarm, (**f**) packing concentration, and (**g**) sum abundance. All variables were transformed using the $\log_{10}$ function as most characteristics showed a log-normal distribution. Note that (**f**,**g**) are not directly comparable to Tarling et al. [16].

The average density of krill in each five-degree longitude sector from the surveyed area showed high densities of krill located in the Ross Sea (170–165° W), followed by areas of low krill densities, and areas of no krill up until the Amundsen Sea (130–120° W), where krill density was the highest in the surveyed area (Figure 5). It then decreased from the Bellingshausen Sea (60–100° W) through Drake's Passage, and there were then instances of increased density of krill again around South Georgia and South Sandwich (25–55° W) (Figure 5).

3.2. Statistical Comparison of Krill Swarm Characteristics

The means and distributions of the swarm characteristic data (depth, thickness, length, area, distance to next warm, packing concentration and sum abundance) extracted from the ACE acoustic data were compared to those reported by Tarling et al. [16] (Figure S2).

The unpaired two-sample *t*-tests showed significant differences between the ACE swarm descriptors and Tarling data for all the descriptors ($p < 0.001$). KS tests showed that there were significant differences between our data and those of Tarling ($p < 0.001$), suggesting that the data distributions are different. However, using a Cohen D test to compare the means of each ACE variable with that of Tarling et al. [16] gave a value of 0.002 for depth, 0.56 for thickness, 0.20 for length, 0.16 for area, 4.67 for distance, 2.66 for packing concentration, and 1.22 for sum abundance. Since Cohen suggests that d = 0.2 is a 'small' effect size, 0.5 is a 'medium' effect size, and 0.8 is a 'large' effect size, these results suggest there is little evidence for a difference between the Tarling et al. [16] and ACE swarm areas or depths, but there was a large difference in their packing concentrations and abundances.

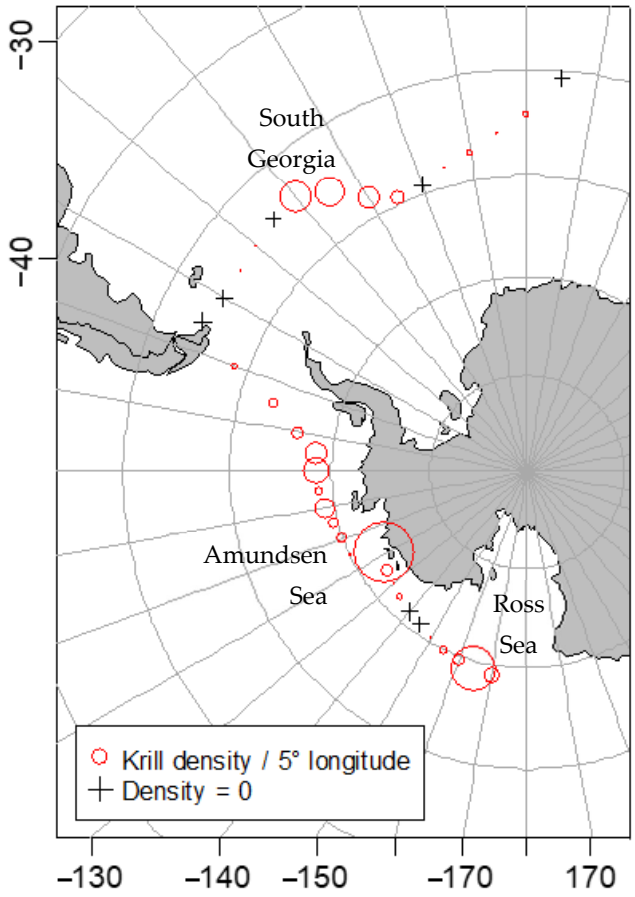


Figure 5. A map of the Southern Ocean showing average krill density (n·m^{-2}) per 5° longitude. Data were collected from 170° W to 18° E. Latitudes and longitudes expressed as negative degrees for west and south.

3.3. Cluster Analysis

The cluster analysis using the swarm characteristics volume backscattering strength, depth, thickness, length, area, distance to next swarm, packing concentration, and sum abundance determined that the most appropriate number of groupings for the krill swarm data was four. These clusters were designated as "Small", "Large", "Shallow", and "Deep". All clusters had a very similar number of swarms, with the largest being n = 556 and the smallest being n = 317. The Euclidean distance was used as the distance metric to determine cluster similarity (Figure S3). Small swarms were the most different from the other three groups, and deep swarms and shallow swarms were the most similar to each other, with large swarms being more similar to the latter two groups than to the small swarm group.

The swarm parameters for each group were illustrated with comparative plots of their statistical distributions (Figure 6). Small swarms contained the smallest of the swarms, as well as the swarm with the shortest length (0.12 m) and smallest area (0.05 m^2). Large swarms had the highest average values in the parameters linked to size, as well as the greatest length (6742.38 m) and largest area (104,776.45 m^2). Large swarms were also the most isolated, with the greatest average distance to neighbour of 14.42 km. Deep swarms had a mean depth of 51.79 m, as well as the densest average packing concentration (2151.30 ind·m^{-3}) and the greatest average sum abundance (569,020.30 ind·m^{-1}). Shallow swarms had a mean depth of 27.72 m and the shallowest individual swarm (15.46 m). They also contained the most sparsely packed swarms with a mean packing concentration of 52.67 ind·m^{-3} and the swarms that were least abundant with a mean sum abundance of 4049.18 ind·m^{-1}. All summary statistics can be found in Table 1.

Linear regression between krill swarm packing concentration and depth resulted in a significant positive relationship ($F(1, 1712) = 957.7$, $p < 0.001$) (Figure S4), with an R^2 value of 0.36 (suggesting 36% of the variation in packing concentration was explained by depth).

Figure 7 is a schematic cartoon showing a typical swarm from each group. Although the groups were associated with a characteristic, e.g., 'deep' or 'large', swarm names were only one of many distinguishing features, as the names simply describe the most prominent distinguishing feature of that group.

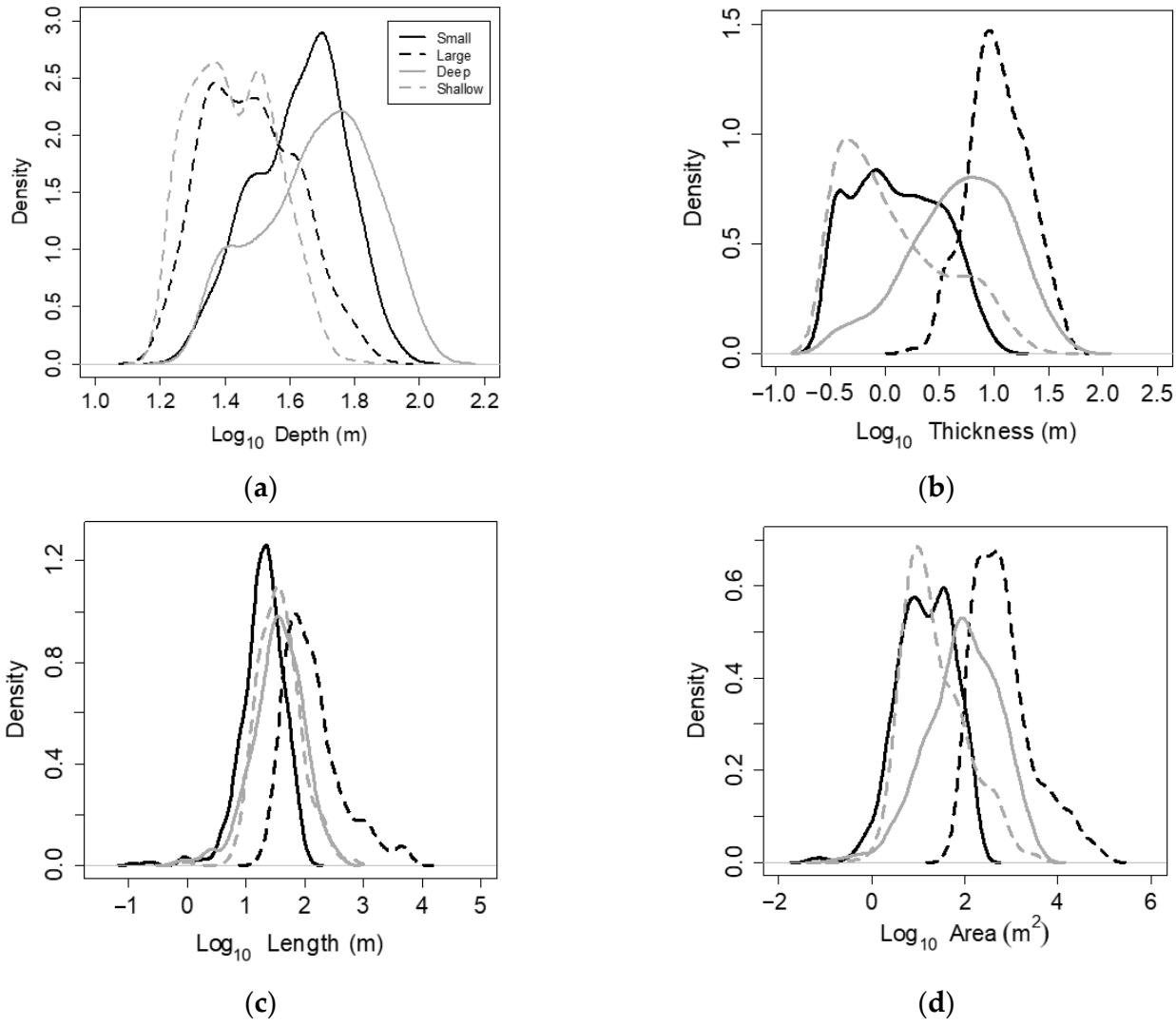
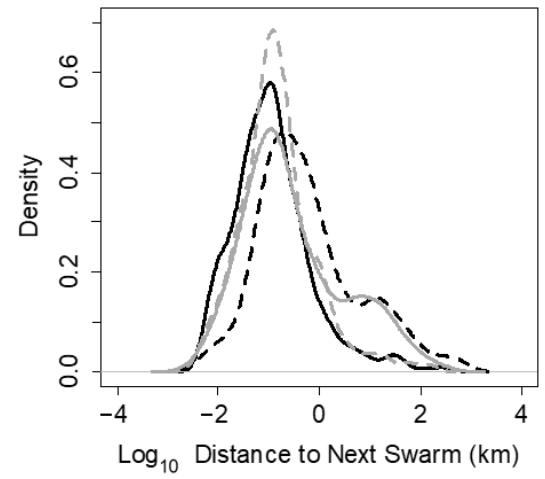
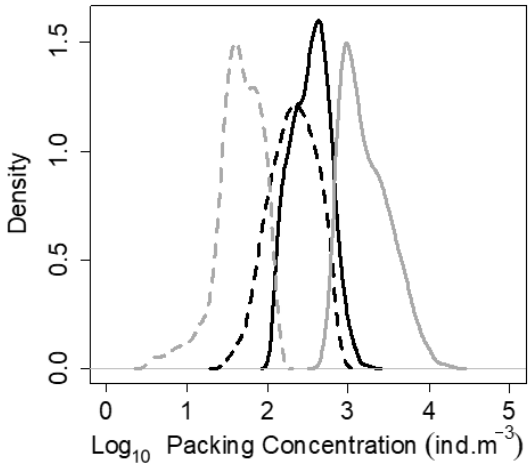


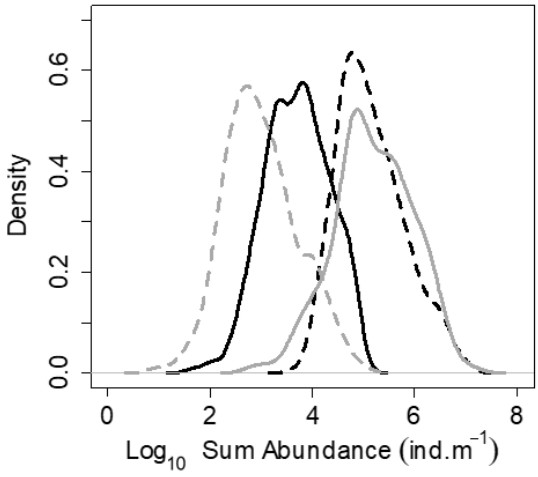
Figure 6. *Cont.*



(**e**)



(**f**)



(**g**)

Figure 6. The density distributions of swarm parameters (on a $\log_{10}$ scale) in different swarm types as determined by the cluster analysis. Graphs show the density distribution of (**a**) swarm depth, (**b**) swarm thickness, (**c**) swarm length, (**d**) swarm area, (**e**) distance to next swarm, (**f**) packing concentration, and (**g**) sum abundance. Solid black line = small swarms; dashed black line = large swarms; solid grey line = deep swarms; dashed grey line = shallow swarms). Note that (**f**,**g**) are not directly comparable to Tarling et al. [16].

These krill swarm groups exhibited differences in their spatial distribution (Figure 8). Deep swarms and shallow swarms had irregular distributions across the study area. They both had high abundances around South Georgia and relatively low abundances elsewhere. Both small swarms and large swarms were relatively evenly distributed across the survey area, with consistently high abundances around South Georgia and in the Ross Sea. Particularly for the smaller swarms, the abundance was slightly higher in both the Bellingshausen and Amundsen Sea than in the Ross Sea and around South Georgia. East of Chile, there was a large stretch of the water in which no krill swarms were located until high densities of swarms from all groups were detected around South Georgia.

Table 1. The characteristics of the four krill swarm types determined using a hierarchical cluster analysis of swarm characteristics. The bottom row shows the statistics for all the swarms in the dataset.

Swarm Type	*N*	Statistic	Volume Backscattering Strength (*Sv*, dB)	Swarm Depth (m)	Swarm Thickness (m)	Swarm Length (m)	Swarm Area (m^2)	Distance to Next Swarm (km)	Packing Concentration (*Nv*, ind·m^{-3})	Sum Abundance (*Nt*, ind·m^{-1})
1 (Small)	556	arithmetic mean	−49.22	44.5	1.92	25.2	31.1	2.4	390.1	12,230.0
		geometric mean	NA	42.3	1.28	19.0	14.7	0.1	340.0	4984.6
		minimum	−53.58	18.0	0.35	0.1	0.1	0.01	124.8	43.2
		maximum	−42.22	89.9	10.01	114.0	198.5	353.3	1703.1	93,229.6
2 (Large)	432	arithmetic mean	−51.41	31.8	13.15	340.9	3173.4	14.4	251.3	481,549.9
		geometric mean	NA	30.1	10.88	133.9	665.4	0.6	205.5	136,727.8
		minimum	−59.38	15.5	1.67	16.8	46.7	0.01	32.8	4734.9
		maximum	−45.97	73.1	44.95	6742.4	104,776.5	661.1	718.2	9,670,024.8
3 (Deep)	317	arithmetic mean	−42.33	51.8	7.91	53.2	293.3	5.8	2151.3	569,020.3
		geometric mean	NA	48.1	4.89	36.1	91.2	0.3	1661.6	151,602.1
		minimum	−46.96	20.4	0.35	0.7	0.2	0.01	572.0	714.3
		maximum	−32.49	105.9	46.55	372.5	3099.2	271.2	16,016.5	12,795,115.3
4 (Shallow)	436	arithmetic mean	−58.08	27.7	2.34	54.5	99.0	2.1	52.7	4,049.2
		geometric mean	NA	26.6	1.18	36.1	22.7	0.2	44.3	1004.5
		minimum	−68.81	15.5	0.35	0.7	0.4	0.01	3.7	7.8
		maximum	−53.56	62.3	23.91	751.4	3287.2	163.3	125.2	97,511.9
All swarms	1741	arithmetic mean	−50.73	38.5	5.90	116.0	875.5	5.8	591.8	228,015.1
		geometric mean	NA	35.4	2.72	40.3	58.8	0.2	240.4	14,135.7
		minimum	−68.81	15.5	0.35	0.1	0.1	0.01	3.7	7.8
		maximum	−32.49	105.9	46.55	6742.4	104,776.5	661.1	16,016.5	12,795,115.3

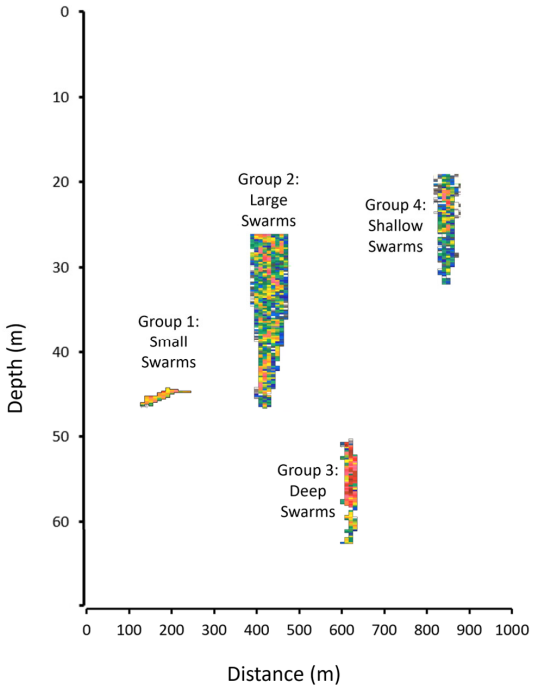


Figure 7. A schematic cartoon showing a typical swarm from each group. Each swarm is scaled appropriately. The typical swarms for Large and Small were based on the average areas for those groups, while the typical swarms for Deep and Shallow were based on the average depths for those groups. Colour scale follows that of Figure 2.

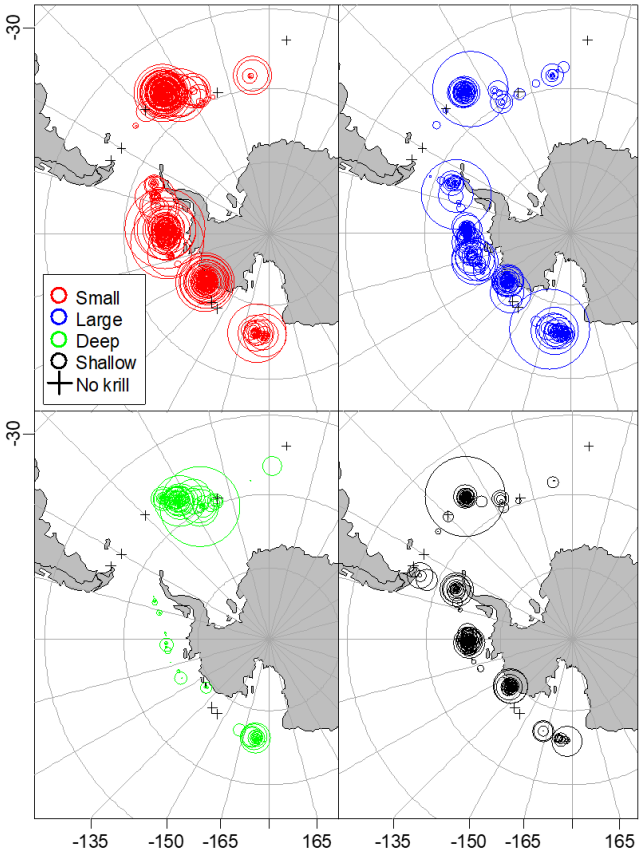


Figure 8. A map of the Southern Ocean showing the abundance and distribution of Antarctic krill swarms (circles proportional to the maximum value of the Nautical Area Scattering Coefficient as a proxy for krill abundance).

3.4. Methane Concentration

The methane concentrations recorded during this study ranged from around 1.77 to 1.82 ppm. These values do not appear to coincide with the increasing krill densities in the area, with areas in which krill density is zero showing the full range of methane concentrations (Figure S5). Given the high zero inflation and skewed nature of the data, a Spearman rank correlation test was used to test the relationship between methane concentration and krill density, revealing a significant but weak negative relationship ($S = 4.394 \times 1011$, $rho = -0.025$, $p = 0.003$).

3.5. Day/Night Differences

The night and day effect, as analysed by the sun angle, was investigated in relation to the various swarm characteristics of interest. Deep swarms were more frequently detected during the day, and these swarms were also more densely packed. Shallow swarms were generally more sparsely packed.

4. Discussion

4.1. Spatial Distribution

High densities of krill were found in the Amundsen Sea. In an examination of over 8000 net samples previously sourced over a period from 1926 to 2004, Atkinson et al. (2008) suggested that there was a relatively low density of Antarctic krill in the Amundsen Sea [28]. This area has historically had a relatively low sampling effort. Our synoptic study suggests that there are relatively high densities of Antarctic krill in this area relative to other areas, contrary to what has previously been found. Projections of krill distributions in the light of climate change, and the associated sea-ice loss, suggest that this will be an area of successful spawning for krill, and our results suggest that this could already be happening even though sea-ice loss is not yet as severe as predicted [11].

Aside from this, the spatial distribution of krill showed similar trends to what would be expected, with higher densities in the areas around South Georgia and swarms present out at sea, away from sea-ice. Our survey was conducted in summer; in winter (June–August), it would be expected that, due to their winter diet of primarily sea-ice algae [29], Antarctic krill would be located in higher densities near this food source. During the summer months (December–February), when there is more sunlight and sea-ice retreats, krill primarily feed on phytoplankton that grows near the surface of the water. The phytoplankton blooms during this time provide a rich and abundant food source for krill [30]. Several other interacting factors can also influence the spatial distribution of krill. These include other physical factors, such as currents [31] and fronts [32]; other biological factors, such as predation [6,9,33,34]; and anthropogenic factors, such as climate change [29].

4.2. Swarm Characteristics

This study investigated Antarctic krill swarms in the Southern Ocean and categorised them based upon a set of defining swarm parameters. A key finding was that the swarms that were most densely packed and most abundant with krill were found in the deepest waters, while the least densely packed swarms that were less abundant with krill were found in shallower waters. It has been stated in previous studies that during the day, krill swarms pack tightly and migrate to deeper depths, while at dusk, swarms migrate to shallower depths where they then disperse [35]. This is supported by the results of this study, as it was found that the deep swarms were tightly packed and more frequently found during the day, and the shallow swarms were more sparsely packed. Tarling et al. [16] found that the swarms that were most densely packed were those of juveniles and the least densely packed swarms typically contained predominantly adult krill [16]. It could be

that the juvenile krill are found deeper in the water column to favour decreased predation pressure over increased food availability. Krill located in deeper water experience much lower predation pressure than those at the surface due to many krill-consuming predators being located near the surface [33]. Atkinson et al. (2008) found that 90% of their surveyed swarms were found in deep water as opposed to shallow water, also possibly due to predator avoidance [28].

The largest swarms also demonstrated the largest distance to the next swarm, while the smallest swarms had a much shorter distance to the next swarm. The smaller swarms that exist more closely to one another were the most frequently observed in this study, while the larger, more isolated swarms were rarer. It has been found previously that krill swarms are present in dense swarms during the day and scatter when it becomes dark [35]. It could be the case that when night comes, the large swarms disperse into smaller swarms, some of which persist as individual swarms located closer to one another that are more frequently observed. On the other hand, it could be the case that a predation event causes this scattering and the subsequent establishment of smaller swarms [34]. Another potential explanation is that although large swarms limit predation by smaller predators that may pick out individuals, it may make them more prone to predation by groups of predators such as seabirds due to the swarms' large size, which allows for easy detection [36]. This, in turn, may cause a lower abundance of large swarms. Another factor to consider is that the results are based on an echosounder that generates a two-dimensional view of a potentially complex three-dimensional structure. As such, one school with amoeboid arms may, in this case, be detected as two separate swarms [6].

Studying swarm characteristics is paramount in unearthing trends that exist in the structure of these swarms in the ocean. It can better help us to understand the potential impacts of climate change on the populations and the consequences on the predators that rely upon them, as their variability can help to predict populations of other species over time. A previous study investigated the characteristics of krill swarms in relation to aggregating Antarctic blue whales and found that these whales associate differently with krill swarms of different characteristics [37]. Studying these swarms can also aid fisheries management in the determination of catch limits, regulating how much krill is removed from the Southern Ocean and mitigating the effects that they have on the structure of the Southern Ocean ecosystem.

4.3. Methane Concentration

Methane production in the marine environment was thought to be a strictly anaerobic process confined primarily to anoxic sediments. However, observations of the supersaturation of methane in oxygenated waters—the 'oceanic methane paradox'—indicates that methane can be produced under oxic conditions, although the mechanisms are unclear [38]. It has been suggested that the grazing processes of krill feeding on phytoplankton, as well as their excretion of faecal pellets, might contribute to microbial methanogenesis and may result in an increase in methane concentration [39,40]. Laboratory experiments have demonstrated the production of methane associated with copepod grazing on phytoplankton in seawater [41], which was postulated to occur in anoxic microniches within the copepod guts or in particles. Field observations have also confirmed the contribution that zooplankton make to oceanic methane [42].

Making use of the interdisciplinary nature of the ACE cruise, with rare simultaneous in situ measurements of both krill and methane, we hypothesised, therefore, that methane levels would be elevated in areas where krill was found due to their combined metabolism in the large and dense swarms. However, our analysis indicated that there was a weak negative relationship between krill density and methane concentration. There are other

sources of methane production in the ocean that may overshadow the potential effect from krill, including methane seepage from patches of high-level organic matter decomposition and the metabolism of other species present alongside krill in the Southern Ocean [43,44]. Zooplankton, for example, are not only more numerous than krill but also more productive: Voronina [45] estimated the total annual methane production of copepods alone at 2,534,106 t and that of krill as 215,106 t (fresh mass). It is possible that, due to the instantaneous nature of both methane data collection and the krill swarm detection, the deep swarms are less likely to be linked to the atmospheric methane concentration, and these are the swarms that are known to be much denser and more likely to produce a recognisable amount of methane. There will be a temporal decoupling between the production of methane by these deep, dense krill swarms and the likelihood of the detection of that methane by the apparatus used here. This is due to the dissolution and dissipation of methane between the swarm and the sea surface, as well as the movement of the water column and the swarm itself, meaning that by the time any methane produced by these swarms reaches the surface it may no longer be representative of the krill swarms that produced it. Finally, as previous evidence suggested that methane was only produced during grazing [41], it could be that many of the krill swarms detected were not feeding, which is likely to be the case for krill detected by day. However, we found no difference in the relationship when considering krill swarms detected by day or night.

4.4. Comparison of Swarm Statistics

To assist in determining that swarms detected during the ACE were composed of Antarctic krill, the statistics were compared with the published statistics from known krill swarms [16]. *t*-tests suggested that there were significant differences between our data and those of Tarling, but these were probably due to the very large and unequal sample sizes. When the data were plotted alongside one another, there was very little difference between the two groups (Figure S2). The Cohen D test further implied that there is not a significant difference between the Tarling and ACE statistics for many of the parameters, as the values were much lower than what would be expected given the results of the *t*-test.

The packing concentrations and sum abundances of the swarms from this study were the only variables that showed a marked difference between the ACE data and those from Tarling's study. This is most likely due to calibration issues or differences in the assumed krill length. The calibration was carried out using standard protocols, and when the calibrated gain values were implemented, we found the integrated value of the sphere to be within 1% of the expected value (theoretical NASC of 1345.81 $m^2 \cdot nmi^{-2}$, c.f. measured NASC 1349 $m^2 \cdot nmi^{-2}$). However, the pre-calibrated NASC measurement was 3.5, leading to a calibrated transducer gain setting of 3.24 dB (with an s_A correction of −1.13), which is very low for such systems, suggesting that the sensitivity was quite low. The study also had no solid ground truthing associated with these swarms, apart from a sample of krill regurgitated by a seabird, so the assumed body length may not have been representative of the krill in the swarms recorded. In order to make the values equivalent to Tarling et al. [16], for example, an increase of 12 dB would be required. Therefore, our results on krill packing density and abundance serve only as relative indices for the purposes of this study and should not, therefore, be considered absolute estimates to be compared with other studies. All of the other swarm parameters would not be affected by calibration errors and are, therefore, comparable.

4.5. Cluster Analysis

The cluster analysis provided four primary swarm groupings based on multiple different factors. While these groups are difficult to summarise based on a single physical

characteristic, clustering in this manner is an effective way to make sense of a complex multi-variate dataset. In particular, active acoustic data analysis provides information-rich data on the physical properties of such targets. Clustering based on a large number of these properties is an invaluable tool for highlighting patterns and commonalities between such groups that are not apparent from standard uni-variable data exploration. This helps to identify differences between the swarms other than just size (e.g., Tarling et al. [16], where size and packing concentration were the main factors used for determining the clusters).

4.6. Data Collection

A final limitation associated with the method of data collection used here is that the accepted method of krill identification described by Watkins and Brierley [22] was unable to be used in a quantitative manner. This is because the 200 kHz and 12.5 kHz echosounders could not be synchronised and, thus, could not be accurately compared with one another for using the decibel difference method. Instead, we had to analyse the swarm data qualitatively by inspection (Figure 3). So, it is possible that some of these may have been misidentified. The effect of this, however, will have been offset by the removal of extreme values during data analysis. The comparison of the final swarm characteristics with those of Tarling (see Section 4.4 above and Figure S2) provided confidence that the krill swarms that we detected were composed of Antarctic krill.

5. Conclusions

Overall, this study provides further insight into the synoptic spatial distribution of Antarctic krill swarms in the Southern Ocean. Antarctic krill were present in high densities in an area not commonly acknowledged, the Amundsen Sea, and this study describes detailed statistics of swarms from a much larger range than previously studied. This study investigated multiple different swarm characteristics and clustered swarms based on these. The outcome of the analysis of swarm characteristics and different swarm types aligned with what has been previously found in relation to the day and night behaviours of krill swarms, providing a large amount of evidence that krill pack tightly and descend to the depths during the day, while at night, they ascend and disperse into smaller, less tightly packed swarms. This study did not determine the relationship between krill density and methane to be positive; in fact, a marginally negative relationship was found. However, the mechanisms by which this relationship was tested meant that a large amount of dispersal may have occurred, causing a temporal and/or spatial mismatch in the datasets, meaning that any relationship was not detectable by the methods used here. In general, this study highlights the benefits of grouping swarms based on their characteristics to better understand their distribution and densities in the Southern Ocean.

Supplementary Materials: The following supporting information can be downloaded at https://www.mdpi.com/article/10.3390/oceans6040063/s1. Figure S1: An image of krill regurgitated from a seabird with an object of a known size used to estimate the average body length of krill. This was then used in determining packing concentration (N_v) and sum abundance (N_t) for individual swarms. Figure S2: Boxplots showing the distribution of swarm characteristics comparing the ACE and Tarling swarm parameter data. All variables were transformed using the $\log_{10}$ function. Note that (**f**) and (**g**) are not directly comparable to Tarling. Figure S3: A dendrogram showing the relative level of similarity between the krill swarms as determined by the descriptors used in the hierarchical cluster analysis. The red boxes represent the groupings, i.e., Group 1, 2, 3 and 4, respectively. Figure S4: The relationship between the depth and packing concentrations of the krill swarms identified on the ACE. Both variables were transformed using the $\log_{10}$ function. Figure S5: The relationship between methane concentration and the density of krill.

Author Contributions: Conceptualisation, A.S.B. and P.G.F.; methodology, A.S.B., P.G.F., J.M.L., I.E., and R.P.; software, M.T. and P.G.F.; formal analysis, M.T.; resources, A.S.B. and P.G.F.; writing—original draft preparation, M.T.; M.B. installed, tested and troubleshooted the acoustic system; writing—review and editing, all authors.; supervision, P.G.F.; project administration, A.S.B. and P.G.F.; funding acquisition, P.G.F. and A.S.B. All authors have read and agreed to the published version of this manuscript with the exception of A.S.B., who saw and approved an earlier draft but has since died.

Funding: The ACE was a scientific expedition carried out under the auspices of the Swiss Polar Institute, supported by funding from the ACE Foundation and Ferring Pharmaceuticals.

Institutional Review Board Statement: Not applicable.

Informed Consent Statement: Not applicable.

Data Availability Statement: The data presented in this study are available on request from the corresponding author. Data are not publicly available as they are still in use by the authors, with the exception of the methane data, which are available at https://doi.org/10.5281/zenodo.2636778.

Acknowledgments: We thank the crew and officers of R/V Akademik Tryoshnikov for their logistic help and support before and during fieldwork. Julia Schmale, of the EPFL Valais Wallis Extreme Environments Research Laboratory (EERL) in SWITZERLAND, provided the methane data. This paper is dedicated to the memory of Andrew Brierley: son, father, partner, mentor, sportsman, marine ecologist of global repute, and dear friend to many of the authors.

Conflicts of Interest: Author Matteo Bernasconi was employed by the company Whales & Co. LLC. The remaining authors declare that the research was conducted in the absence of any commercial or financial relationships that could be construed as a potential conflict of interest.

Abbreviations

The following abbreviations are used in this manuscript:

ACC	Antarctic Circumpolar Current
ACE	Antarctic Circumnavigation Expedition
CCAMLR	Commission for the Conservation of Antarctic Marine Living Resources
EDSU	Equivalent Distance Sampling Unit
KS	Kolmogorov–Smirnov
Nt	Sum Abundance
Nv	Packing Concentration
PAR	Photosynthetically Active Radiation
Sv	Volume Backscattering Strength
TS	Target Strength

References

1. Hill, S.L.; Murphy, E.J.; Reid, K.; Trathan, P.N.; Constable, A.J. Modelling Southern Ocean ecosystems: Krill, the food-web, and the impacts of harvesting. *Biol. Rev.* **2006**, *81*, 581–608. [CrossRef]
2. Meyer, B.; Atkinson, A.; Bernard, K.S.; Brierley, A.S.; Driscoll, R.; Hill, S.L.; Marschoff, E.; Maschette, D.; Perry, F.A.; Reiss, C.S.; et al. Successful ecosystem-based management of Antarctic krill should address uncertainties in krill recruitment, behaviour and ecological adaptation. *Commun. Earth Environ.* **2020**, *1*, 28. [CrossRef]
3. Everson, I. Managing Southern Ocean krill and fish stocks in a changing environment. *Philos. Trans. R. Soc. London Ser. B* **1992**, *338*, 311–317. [CrossRef]
4. Constable, A.J.; de la Mare, W.K.; Agnew, D.J.; Everson, I.; Miller, D. Managing fisheries to conserve the Antarctic marine ecosystem: Practical implementation of the Convention on the Conservation of Antarctic Marine Living Resources (CCAMLR). *ICES J. Mar. Sci.* **2000**, *57*, 778–791. [CrossRef]
5. Watkins, J.L.; Morris, D.J.; Ricketts, C.; Priddle, J. Differences between swarms of Antarctic krill and some implications for sampling krill populations. *Mar. Biol.* **1986**, *93*, 137–146. [CrossRef]

6. Brierley, A.S.; Cox, M.J. Shapes of Krill Swarms and Fish Schools Emerge as Aggregation Members Avoid Predators and Access Oxygen. *Curr. Biol.* **2010**, *20*, 1758–1762. [CrossRef] [PubMed]
7. Tynan, C.T. Ecological importance of the Southern Boundary of the Antarctic Circumpolar Current. *Nature* **1998**, *392*, 708–710. [CrossRef]
8. Quetin, L.B.; Ross, R.M.; Fritsen, C.H.; Vernet, M. Ecological responses of Antarctic krill to environmental variability: Can we predict the future? *Antarct. Sci.* **2007**, *19*, 253–266. [CrossRef]
9. Nowacek, D.P.; Friedlaender, A.S.; Halpin, P.N.; Hazen, E.L.; Johnston, D.W.; Read, A.J.; Espinasse, B.; Zhou, M.; Zhu, Y. Super-Aggregations of Krill and Humpback Whales in Wilhelmina Bay, Antarctic Peninsula. *PLoS ONE* **2011**, *6*, e19173. [CrossRef]
10. Lascara, C.M.; Hofmann, E.E.; Ross, R.M.; Quetin, L.B. Seasonal variability in the distribution of Antarctic krill, *Euphausia superba*, west of the Antarctic Peninsula. *Deep Sea Res. Part I* **1999**, *46*, 951–984. [CrossRef]
11. Piñones, A.; Fedorov, A.V. Projected changes of Antarctic krill habitat by the end of the 21st century. *Geophys. Res. Lett.* **2016**, *43*, 8580–8589. [CrossRef]
12. Hobbs, W.R.; Massom, R.; Stammerjohn, S.; Reid, P.; Williams, G.; Meier, W. A review of recent changes in Southern Ocean sea ice, their drivers and forcings. *Glob. Planet. Change* **2016**, *143*, 228–250. [CrossRef]
13. Hofmann, E.E.; Murphy, E.J. Advection, Krill, and Antarctic Marine Ecosystems. *Antarct. Sci.* **2004**, *16*, 487–499. [CrossRef]
14. Zhou, M.; Dorland, R.D. Aggregation and vertical migration behavior of *Euphausia superba*. *Deep Sea Res. Part II* **2004**, *51*, 2119–2137. [CrossRef]
15. Krafft, B.A.; Skaret, G.; Knutsen, T.; Melle, W.; Klevjer, T.; Søiland, H. Antarctic krill swarm characteristics in the Southeast Atlantic sector of the Southern Ocean. *Mar. Ecol. Prog. Ser.* **2012**, *465*, 69–83. [CrossRef]
16. Tarling, G.A.; Klevjer, T.; Fielding, S.; Watkins, J.; Atkinson, A.; Murphy, E.; Korb, R.; Whitehouse, M.; Leaper, R. Variability and predictability of Antarctic krill swarm structure. *Deep Sea Res. Pt I* **2009**, *56*, 1994–2012. [CrossRef]
17. Brinton, E.; Antezana, T. Structures of Swarming and Dispersed Populations of Krill (*Euphausia superba*) in Scotia Sea and South Shetland Waters During January-March 1981, Determined by Bongo Nets. *J. Crustac. Biol.* **1984**, *4*, 45–66. [CrossRef]
18. Heywood, R.B.; Everson, I.; Priddle, J. The absence of krill from the South Georgia zone, winter 1983. *Deep Sea Res. Pt A* **1985**, *32*, 369–378. [CrossRef]
19. Siegel, V. *A Concept of Seasonal Variation of Krill (Euphausia superba) Distribution and Abundance West of the Antarctic Peninsula. Antarctic Ocean and Resources Variability*; Sahrhage, D., Ed.; Springer: Berlin/Heidelberg, Germany, 1988; pp. 219–230. [CrossRef]
20. Siegel, V.; Bergström, B.; Strömberg, J.O.; Schalk, P.H. Distribution, size frequencies and maturity stages of krill, *Euphausia superba*, in relation to sea-ice in the Northern Weddell Sea. *Polar Biol.* **1990**, *10*, 549–557. [CrossRef]
21. Simmonds, E.J.; MacLennan, D.N. *Fisheries Acoustics: Theory and Practice*, 2nd ed.; Blackwell Publishing Limited: Oxford, UK, 2005; pp. 70–126. [CrossRef]
22. Watkins, J.L.; Brierley, A.S. Verification of the acoustic techniques used to identify Antarctic krill. *ICES J. Mar. Sci.* **2002**, *59*, 1326–1336. [CrossRef]
23. Foote, K.G.; Knudsen, H.P.; Vestnes, G.; MacLennan, D.N.; Simmonds, E.J. Calibration of Acoustic Instruments for Fish Density Estimation: A Practical Guide. *ICES Coop. Res. Rep.* **1987**, *144*, 84.
24. Demer, D.A.; Berger, L.; Bernasconi, M.; Bethke, E.; Boswell, K.; Chu, D.; Domokos, R.; Dunford, A.; Fässler, S.; Gauthier, S.; et al. Calibration of acoustic instruments. *ICES Coop. Res. Rep.* **2015**, *326*, 136.
25. Coetzee, J. Use of a shoal analysis and patch estimation system (SHAPES) to characterise sardine schools. *Aquat. Living Resour.* **2000**, *13*, 1–10. [CrossRef]
26. Cohen, J. *Statistical Power Analysis for the Behavioral Sciences*, 2nd ed.; Routledge Academic: New York, NY, USA, 1988. [CrossRef]
27. Nielsen, F. Hierarchical Clustering. In *Introduction to HPC with MPI for Data Science*; Springer: Berlin/Heidelberg, Germany, 2016; pp. 195–211. [CrossRef]
28. Atkinson, A.; Siegel, V.; Pakhomov, E.A.; Rothery, P.; Loeb, V.; Ross, R.M.; Quetin, L.B.; Schmidt, K.; Fretwell, P.; Murphy, E.J.; et al. Oceanic circumpolar habitats of Antarctic krill. *Mar. Ecol. Prog. Ser.* **2008**, *362*, 1–23. [CrossRef]
29. Flores, H.; Atkinson, A.; Kawaguchi, S.; Krafft, B.A.; Milinevsky, G.; Nicol, S.; Reiss, C.; Tarling, G.A.; Werner, R.; Rebolledo, E.B.; et al. Impact of climate change on Antarctic krill. *Mar. Ecol. Prog. Ser.* **2012**, *458*, 1–19. [CrossRef]
30. Atkinson, A.; Siegel, V.; Pakhomov, E.; Rothery, P. Long-term decline in krill stock and increase in salps within the Southern Ocean. *Nature* **2004**, *432*, 100–103. [CrossRef]
31. Annasawmy, P.; Horne, J.K.; Reiss, C.S.; Cutter, G.R.; Macaulay, G.J. Antarctic krill (*Euphausia superba*) distributions, aggregation structures and predator interactions in Bransfield Strait. *Polar Biol.* **2023**, *46*, 151–168. [CrossRef]
32. Kasyan, V.V. Age Structure and Spatial Distribution of *Euphausia superba* Larvae off the Antarctic Peninsula, Southern Ocean. *Water* **2022**, *14*, 3196. [CrossRef]
33. Hunt, G.L.; Heinemann, D.; Everson, I. Distributions and predator-prey interactions of macaroni penguins, Antarctic fur seals, and Antarctic krill near Bird Island, South Georgia. *Mar. Ecol. Prog. Ser.* **1992**, *86*, 15–30. [CrossRef]

34. Cox, M.J.; Demer, D.A.; Warren, J.D.; Cutter, G.R.; Brierley, A.S. Multibeam echosounder observations reveal interactions between Antarctic krill and air-breathing predators. *Mar. Ecol. Prog. Ser.* **2009**, *378*, 199–209. [CrossRef]
35. Everson, I. Diurnal variations in mean volume backscattering strength of an Antarctic krill (*Euphausia superba*) patch. *J. Plankton Res.* **1982**, *4*, 155–162. [CrossRef]
36. Nevitt, G. Olfactory foraging in Antarctic seabirds: A species-specific attraction to krill odors. *Mar. Ecol. Prog. Ser.* **1999**, *177*, 235–241. [CrossRef]
37. Miller, E.J.; Potts, J.M.; Cox, M.J.; Miller, B.S.; Calderan, S.; Leaper, R.; Olson, P.A.; O'Driscoll, R.L.; Double, M.C. The characteristics of krill swarms in relation to aggregating Antarctic blue whales. *Sci. Rep.* **2019**, *9*, 1–13. [CrossRef]
38. Bižić, M.; Grossart, H.-P.; Ionescu, D. Methane Paradox. In *eLS*; John Wiley & Sons, Ltd.: Chichester, UK, 2020; pp. 1–11. [CrossRef]
39. Yoshida, O.; Inoue, H.Y.; Watanabe, S.; Suzuki, K.; Noriki, S. Dissolved methane distribution in the South Pacific and the Southern Ocean in austral summer. *J. Geophys. Res. Ocean.* **2011**, *116*, 1–9. [CrossRef]
40. Boontanon, N.; Watanabe, S.; Odate, T.; Yoshida, N. Methane production, consumption and its carbon isotope ratios in the Southern Ocean during the austral summer. *Biogeosci. Discuss.* **2010**, *7*, 7207–7225. [CrossRef]
41. de Angelis, M.A.; Lee, C. Methane production during zooplankton grazing on marine phytoplankton. *Limnol. Oceanogr.* **1994**, *39*, 1298–1308. [CrossRef]
42. Schmale, O.; Wäge, J.; Mohrholz, V.; Wasmund, N.; Gräwe, U.; Rehder, G.; Labrenz, M.; Loick-Wilde, N. The contribution of zooplankton to methane supersaturation in the oxygenated upper waters of the central Baltic Sea. *Limnol. Oceanogr.* **2017**, *63*, 412–430. [CrossRef]
43. Römer, M.; Torres, M.; Kasten, S.; Kuhn, G.; Graham, A.; Mau, S.; Little, C.; Linse, K.; Pape, T.; Geprägs, P.; et al. First evidence of widespread active methane seepage in the Southern Ocean, off the sub-Antarctic island of South Georgia. *Earth Planet. Sci. Lett.* **2014**, *403*, 166–177. [CrossRef]
44. Ratnarajah, L.; Bowie, A.R.; Lannuzel, D.; Meiners, K.M.; Nicol, S. The Biogeochemical Role of Baleen Whales and Krill in Southern Ocean Nutrient Cycling. *PLoS ONE* **2014**, *9*, e0125134. [CrossRef]
45. Voronina, N.M. Comparative abundance and distribution of major filter-feeders in the Antarctic pelagic zone. *J. Mar. Syst.* **1998**, *17*, 375–390. [CrossRef]

Disclaimer/Publisher's Note: The statements, opinions and data contained in all publications are solely those of the individual author(s) and contributor(s) and not of MDPI and/or the editor(s). MDPI and/or the editor(s) disclaim responsibility for any injury to people or property resulting from any ideas, methods, instructions or products referred to in the content.